Neurology Asia 2024; 29(1) : 133 – 144

Clinical, neurophysiological and genetic characteristics of Charcot-Marie-Tooth from a research center in northern China

*Jingfei Zhang, *Huiqiu Zhang, Fei Zhao, Xueli Chang, Juan Wang, Jing Zhang, Xiaomin Pang, Jiaying Shi, Junhong Guo, Wei Zhang

*JF Zhang and HQ Zhang contributed equally to this work and are co-first authors

Department of Neurology, First Hospital, Shanxi Medical University, Taiyuan, China

Abstract

Background & Objectives: Charcot-Marie-Tooth (CMT) disease is a group of hereditary sensorimotor neuropathies with a great variability of genotypes and phenotypes. The aims of the study were to provide a general perspective of the clinical manifestations and the frequency of genetic subtypes in CMT patients from a medical center in Taiyuan, northern China. *Methods:* Twenty-eight unrelated CMT patients were enrolled from a research center in northern China according to the CMT diagnosis criteria formulated by De Jonghe *et al*. in 1998. Then multiplex ligation-dependent probe amplification (MLPA) testing combined with next-generation sequencing (NGS) were performed among 18 of these patients. *Results: PMP22* duplications were identified in 8 patients. In addition, 2 novel mutations were detected in the *GJB1* gene (c.236T>C and c.464T>C). According to the American College of Medical Genetics and Genomics (ACMG) standards and guidelines, both two *GJB1* mutations were assigned as 'likely pathogenic'. *PMP22* and *GJB1* were the most common causative genes in CMT1 and intermediate CMT, respectively. In addition, the first CMTX6 patient with a p.R158H mutation in the *PDK3* gene was confirmed in China. Our study further shows that the p.R158H of *PDK3* is likely to be a recurrent mutation.
Conclusions: The results have broadened the genetic and clinical spectrums of CMT patients, which can help facilitate the diagnosis of CMT. Despite the increasing popularity of NGS, genetic screening of large cohorts of CMT patients using NGS is still rarely performed in the Chinese population. In CMT we suggest having MLPA for *PMP22* as the first tier of study followed by target NGS for those with negative MLPA findings. The deciphering of the target gene candidates can further be guided by electromyographic data.

Keywords: Charcot-Marie-Tooth disease, genetic spectrum, clinical profile, *GJB1, PDK3*

INTRODUCTION

Inherited neuropathies represent several common neurological disorders with various clinical manifestations and genetic causes, while Charcot-Marie-Tooth disease (CMT) is the most widely seen inherited neuromuscular disorder with an incidence of approximately 30 in 100,000 individuals. In clinics, the most common features of CMT are deterioration of distal muscle strength, distal muscle atrophy, steppage gait, foot deformities, a decrease or absence of deep-tendon reflexes, and distal sensory loss. From the electrophysiological features, CMT is classified into axonal CMT (MNCV>45m/s), demyelinating CMT (MNCV<25m/s), or intermediate CMT (25m/s<MNCV<45m/s) based on the upper limb motor nerve conduction velocity, in most cases, median motor nerve conduction velocities (MMNCVs). All mendelian inheritance modes have been reported in CMT, including X-linked, autosomal dominant, and autosomal recessive. Although detailed neuromuscular evaluations could assist in CMT identification aside from family history assessments, genetic testing can enable definitive diagnosis of certain CMT subtypes and their related genes. More than 80 CMT-disease-causing genes have been identified (https://neuromuscular.wustl.edu/time/hmsn.html), and such a finding poses a

Address correspondence to: Wei Zhang, Department of Neurology, First Hospital, Shanxi Medical University, No.85, Jiefang South Street, Taiyuan, China. Tel: +8618835166424, E-mail: zhangvey@126.com

Date of Submission: 28 May 2023; Date of Acceptance: 28 November 2023

https://doi.org/10.54029/2024xka

remarkable challenge for genetic testing in CMT patients. Furthermore, the underlying pathogenic mechanisms of these genes remain largely unclear and more corresponding researches are needed.

In this study, 28 independent patients suspected of CMT were enrolled from a research center in Taiyuan, northern China. After clinical and electrophysiological examinations, MLPA testing plus targeted NGS were performed in 18 patients. This study aims to comprehensively analyze these patients' clinical, neurophysiological and genetic spectra.

METHODS

Clinical assessment

Twenty-eight CMT patients (16 males and 12 females) were recruited from the Department of Neurology, the First Hospital of Shanxi Medical University, Shanxi Province, China (our Hospital and Department) from January 2017 to January 2021. Probands were identified at the neurology clinic with standard electrophysiological and clinical evaluations by qualified neurologists. All clinical diagnoses were provided based on previously proposed criteria for CMT diagnosis. The following information of CMT was recorded: family history, age of diagnosis, gender, age of onset, disease duration, site of onset, muscle strength based on Medical Research Council (MRC), areflexia, sensory loss, muscle atrophy, and skeletal deformities. This study was reviewed and approved by the Institutional Ethics Committee of the First Hospital of Shanxi Medical University (Shanxi, China). Informed consent for participation, samples, and medical records were obtained from the participants in person or their guardians.

Electromyography

After detailed clinical history inquiry and physical examination, patients clinically diagnosed as CMT underwent neurophysiological studies. A standard battery of nerve-conduction study including measurements of motor nerve conduction velocity (MNCV), sensory nerve conduction velocity (SNCV), distal motor latency, and F wave latency on the upper and lower limbs (median, ulnar, tibial, and common peroneal nerves) were applied to evaluate demyelination changes of peripheral nerves, sometimes with slight axonal alterations. Sensory nerve action potential amplitude (SNAP) and complex muscle action potential (CMAP) were measured to evaluate peripheral nerve axonal lesions, which mainfested profound reduction in the CMAPs and SNAPs with relative preserved conduction velocities. Needle electromyography was used to observe the electrical potential changes of muscles in the three states of rest, light contraction and strong contraction, so as to help determine whether the damage was neurogenic or myogenic.

MLPA assay, targeted NGS and Sanger sequencing

Peripheral blood samples were collected from the patients, placed in ethylene diamine tetraacetic acid (EDTA) tubes, and stored at -20 °C until use. A CWE9600 Automated Nucleic Acid Extraction System was used to extract DNA using CWE2100 Blood DNA Kit V2 (CWBiotech, China) following the standard protocol. A multiplex ligation-dependent probe amplification (MLPA) kit (MRC Holland, Amsterdam, the Netherlands) was used to observe the duplication or deletion of *PMP22* (MIM# 601097, RefSeq NM_000304.2) following the manufacturer's protocol. If the patients were detected to be MLPA-negative, they were further sequenced on a gene panel of 197 genes known to involve in the pathology of CMT and several other inherited peripheral neuropathies. Quality control for the raw data of targeted NGS was performed with Illumina Sequence Control Software (SCS), and the data were then aligned to the human reference genome (hg19) with the BWA Aligner. Small insertions/deletions (INDELs) and single-nucleotide polymorphisms (SNPs) were analyzed by a Genome Analysis ToolKit (GATK). Variants were marked with ANNOVAR, and those whose quality scores were low (genotype quality < 20 or depth < 10) were filtered. Besides, variants with a minor allele frequency (MAF) > 0.5% in dbSNP, genomeAD, and EXAC were also excluded. SIFT, Polyphen-2, and Mutation Taster programs were applied to predict the pathogenicity of the variants. All of the potential variants were validated by Sanger sequencing and 200 healthy Han Chinese were screened as controls for sequence variants. Upon detection of a sequence variant in the proband, other family members, if available, were analyzed to determine the correlation between the observed variant and the disease.

Molecular modeling and conservative analysis

To evaluate the evolutionary conservativeness of the mutated sites, HomoloGene was used to align the sequences of gap junction beta-1 proteins from multiple animal species. The three-dimensional

structures of mutant and wild-type proteins were constructed with computer modeling and submitted to the Swiss-Model server (https://www.swissmodel.expasy.org) for homology modeling. Subsequently, amino acid changes were evaluated and visualized for their impacts on the protein structure with PyMOL.

Statistical analysis

Statistical analyses were conducted using SPSS version 21.0 (IBM Corp, Armonk, New York). Data with a normal distribution was expressed as the mean ± standard deviation, and that with a non-normal distribution was described as medians (range). Continuous variables were compared by Mann-Whitney U test depending on the distribution and two-tailed $p<0.05$ was considered statistically significant.

RESULTS

Clinical features

Twenty-eight unrelated patients (16 males and 12 females) were recruited in the study. Based on clinical data, especially family history, the numbers of cases considered to be autosomal dominant inherited (AD), X-linked inherited, and sporadic were 12 (42.9%), 3 (10.7%), and 13 (46.4%), respectively. The patients showed a median age of onset of 30.5 years old with a range of 1 to 54 years old. The age at diagnosis ranged from 13 to 75 years old (median was 33.5 years). Specifically, the body parts exhibiting symptoms of weakness at disease onset were the lower limbs (14 patients, 50.0%), the upper limbs (2 patients, 7.1%), and both (5 patients, 17.9%). Five (17.9%) patients started with sensory abnormalities, and the onset symptoms of the remaining 2 patients were unavailable.

Mutation analysis

Of the study patients, 18/28 unrelated patients suspected of CMT recruited in our study were able to undergo genetic testing which included MLPA testing plus targeted NGS, whereas 10/28 of patients did not. *PMP22* duplications were found in 44.4% of the cases (8/18) according to the MLPA findings, and these cases were determined MLPA-positive. The remaining 10 MLPA-negative patients were subject to targeted NGS with a panel of 197 genes that were known to participate in the pathology of CMT and several other inherited peripheral neuropathies (Supplementary Table 1). More than 99.80% of the target bases revealed >20x coverage, and the mean coverage of these targeted bases was 180.67. For the 10 patients with MLPA negative findings, 6/10 of them had NGS positive findings with 4 known pathogenic variants (Table 1) and 2 novel ones (Table 2) were identified. Variants of the *MORC2* (NM_001303256), *MPZ* (NM_000530.6), *SLC12A6* (NM_133647.1), and *PDK3* (NM_001142386.2) genes were respectively identified in 4 cases. Two de novo variants c.464T>C (NM_000166.5) and c.236T>C (NM_004184.3) in the *GJB1* (NM_000166.5) gene, were identified in 2 independent cases. Both the two novel variants co-segregated with the phenotypes, and were seen in neither of the following: Exome Aggregation Consortium (ExAC) database, 1000 Genomes project, dbSNP, ClinVar database, the Genome Aggregation Database (gnomAD), the Human Gene Mutation Database (HGMD), and the healthy controls. Assessments of Mutation Taster, PolyPhen-2, and SIFT suggested that both of them could lead to changes in amino acid sequences that affecting proteins. According to ACMG standards and guidelines, both two were assigned as 'likely pathogenic'. Through Sanger sequencing, they segregated with the clinical phenotypes respectively in families. No variant was observed in the remaining 4 cases. Of these 4 cases, 1 patient had a definite family history. Therefore, the genetic diagnosis rates were 77.8% (14/18) in CMT patients.

Genetic subtypes of CMT patients

Of the 14 patients genetically diagnosed as CMT in this study, 8 patients were categorized as CMT1A due to *PMP22* duplication, 2 patients were identified as CMTX1 with *GJB1* mutations and the other 4 patients carried the corresponding mutations in *MPZ* (CMT1B), *MORC2* (CMT2), *PDK3* (CMTX6), and *SLC12A6*. Partial genetic subtypes are provided in Figure 1.

Genotype-phenotype correlation in CMT patients

The clinical features of the *PMP22*-mutated patients are summarized in Table 1. The median age of onset of 8 CMT1A patients (with *PMP22* duplication) was 40.5 years old, ranging from 13 to 54 years, and 7 of them began with motor symptoms but only 1 started sensory symptoms. Besides, 62.5% of CMT1A patients had positive family histories. 8 (7 unrelated probands and 1 relative) CMT1A patients had electrophysiological

Table 1: Clinical features of CMT patients in the study

Patient ID	Gene	Transcript	CMT subtype	Variants	Amino acid change	Family history	Inheritance pattern	Zygote	Age of onset, y	Age at diagnosis, y	MNCV, m/s	Electro-physiological classification	Associated clinical features	Foot deformity	CMTNSv2
1	*PMP22*	NM_000304.2	CMT1A	Dup 0.031 MB	-	Postive	AD	Het	54	59	30.6	Intermediate	Symmetrical distal extremity weakness and hypoesthesia	N	16
2	*PMP22*	NM_000304.2	CMT1A	Dup 0.031 MB	-	Positive	AD	Het	36	37	20.4	Demyelinating	Muscle fibrillation, tremor, paresthesia	P	2
3	*PMP22*	NM_000304.2	CMT1A	Dup 0.031 MB	-	Negative	De novo	Het	51	58	28.6	Intermediate	Symmetrical distal extremity weakness	/	16
4	*PMP22*	NM_000304.2	CMT1A	Dup 0.031 MB	-	Negative	De novo	Het	39	39	31.6	Intermediate	Symmetrical distal extremity hypoesthesia	/	1
5	*PMP22*	NM_000304.2	CMT1A	Dup 0.031 MB	-	Negative	De novo	Het	23	28	26	Intermediate	Symmetrical distal extremity weakness	/	8
6	*PMP22*	NM_000304.2	CMT1A	Dup 0.031 MB	-	Positive	AD	Het	45	47	20.7	Demyelinating	Symmetrical distal extremity weakness and hypoesthesia, muscle atrophy	P	20
7	*PMP22*	NM_000304.2	CMT1A	Dup 0.031 MB	-	Positive	AD	Het	13	13	21.1	Demyelinating	Symmetrical distal extremity weakness, hypoesthesia of the right lower limb	/	8
8	*PMP22*	NM_000304.2	CMT1A	Dup 0.031 MB	-	Positive	AD	Het	42	44	/	/	Symmetrical distal extremity weakness	P	/
9	*GJB1*	NM_000166.5	CMTX1	c.464T>C	p. L155P	Positive	XD	Hemi	1	17	40.1	Intermediate	Symmetrical distal extremity weakness and hypoesthesia Gait ataxia	P	6
Patient 9's mother	*GJB1*	NM_000166.5	CMTX1	c.464T>C	p. L155P	Positive	XD	Het	20	40	42.6	Intermediate	Gait ataxia	P	12
10	*GJB1*	NM_004184.3	CMTX1	c.236T>C	p. L79P	Positive	XD	Hemi	1	27	37.4	Intermediate	Symmetrical distal extremity weakness and hypoesthesia Gait ataxia Muscle atrophy	P	8
Patient 10's brother	*GJB1*	NM_004184.3	CMTX1	c.236T>C	p. L79P	Positive	XD	Hemi	1	20	/	/	Symmetrical distal extremity weakness and hypoesthesia Gait ataxia Muscle atrophy	/	/

Patient 10's mother	*GJB1*	NM_004184.3	CMTX1	c.236T>C	p. L79P	Positive	XD	Het	1	47	/	/	Gait ataxia	/	/
11	*PDK3*	NM_004184.3	CMTX6	c.473G>A	p. R158H	Positive	XD	Het	14	33	/	/	Symmetrical distal extremity weakness and hypoesthesia,	P	/
12	*MPZ*	NM_000530.6	CMT1B	c.233C>T	p. S78L	Negative	De novo	Het	43	47	26.9	Intermediate	Symmetrical distal extremity weakness and hypoesthesia, Muscle atrophy	P	14
13	*MORC2*	NM_001303256	CMT2	c.1396G>A	p. D466N	Positive	AD	Het	1	26	55.8	Axonal	Symmetrical distal extremity weakness and hypoesthesia,	N	6
14	*SLC12A6*	NM_133647.1	ICMT	c.620G>A	p. R207H	Negative	De novo	Het	27	31	41.0	Intermediate	Symmetrical distal extremity weakness and hypoesthesia, Muscle atrophy	N	19

MNCV=median motor nerve conduction velocity; Foot deformity: P = pes cavus; N = normal; S=Sporadic; Het=heterozygote; Hemi=hemizygote; Electrophysiological classification: demyelinating CMT (MNCV<25m/s), axonal CMT (MNCV >45m/s) and intermediate CMT (25m/s<MNCV<45m/s); / = not available.

Table 2: *GJB1* variants identified in our study

Gene	Nucleotide change	Amino acid change	CMT subtype	1000G	ExAC	Mutation Taster	SIFT	Polyphen-2	ACMG	Family segregation
GJB1	c.236T>C	p. L79P	ICMT	0	0	disease causing	Deleterious	Probably damaging	Likely pathogenic (PM2+PP1/2/3/4)	Yes
GJB1	c.464T>C	p. L155P	ICMT	0	0	disease causing	Neutral	Probably damaging	Pathogenic (PM2+PM5+PP1/2/3/4)	Yes

Abbreviation: 1000G, 1000 Genomes Project; ExAC, Exome Aggregation Consortium; ACMG: the American College of Medical Genetics and Genomics; ICMT=intermediate CMT

data. The median nerve MNCV of the non-dominant upper limbs in 8 patients with CMT1A ranged from 20.4 to 31.6 m/s (mean 24.4), which was classified as intermediate or demyelination. The CMAP amplitudes varied from 0.45 to 10.2 mV (mean 4.2) and a median SNAP in the median nerve was 1.58uV. Moreover, 2 CMT1A patients didn't show median SNAP due to no response to electrophysiological detection. Notably, 50.0% of CMT1 patients demonstrated median nerve MNCVs slower than 25 m/s. The clinical manifestations of patients with *GJB1* gene mutations are presented in Table 1. Patients carrying *GJB1* mutations (2 unrelated probands and 3 relatives) all started with motor symptoms. All the 5 patients with CMT1X complained of gait disorder since childhood including unsteady walking and inability to walk on the heel, and

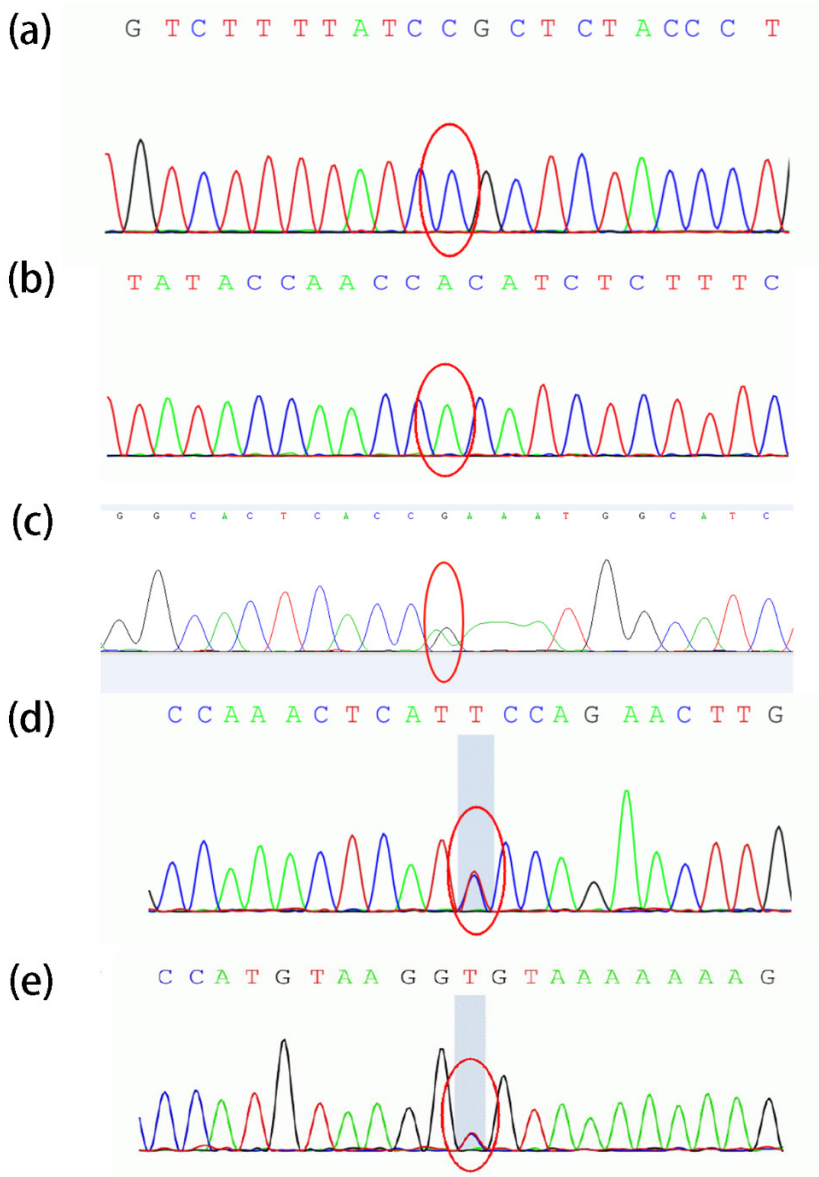

Figure 1. Mutation sequencing results. **a** Hemizygote *GJB1* mutation c.464T>C corresponding to the amino acid substitution Leu155Pro. **b** Hemizygote *PDK3* mutation c.473G>A corresponding to the amino acid substitution Leu155Pro. **c** Hemizygote *MPZ* mutation c.233C>T corresponding to the amino acid substitution Ser78Leu. **d** Hemizygote *MORC2* mutation c.1396G>A corresponding to the amino acid substitution Asp466Asn. **e** Hemizygote *SLC12A6* mutation c.620G>A corresponding to the amino acid substitution Arg207His.

3 of them received EMG detection. Also in Table 3, we showed the electrophysiological data of the two CMT1X patients and the mother of the proband carrying the c.464T>C mutation in the *GJB1* gene. The EMG parameters were similar to the CMT1X EMG detection results related to *GJB1* mutation reported in previous literature (ulnar MNCV range from 33 to 42m/s (mean 38) in male, while from 44 to 56m/s (mean 49) in female). Electrophysiological studies showed a greater median SNAP and an intermediate median MNCV compared to patients with *PMP22* duplications. The non-dominant median nerve MNCV of the CMT1A patients (median 24.4m/s) was significantly lower than that of CMT1X patients (median 40.1m/s) (P=0.014, Mann-Whitney U test, Figure 2). Detailed electrophysiological characteristics of CMT patients carrying *PMP22 (dup)* mutations and novel *GJB1* mutations were presented in Table 3. Clinical features and electrophysiological results of the four patients with *MORC2* (c.1396G>A), *PDK3* (c.794C>T), *SLC12A6* (c.620G>A), and *MPZ* (c.233C>T) mutations were provided in Table 1. It was worth mentioning that we identified the first CMTX6 patient in China, with the same mutation site previously reported. Through Sanger sequencing, the mutation was proved of maternal origin and was heterozygous in the proband's sister. However, the proband's mother and sister were both asymptomatic. The pedigree diagram of the family was showed in Figure 3.

Molecular modeling and conservative analysis

The three-dimensional structural model of Cx32 was predicted by SWISS-MODEL to find out whether the novel p.L79P and p.L155P missense mutations affected the protein structure. Structural templates against the primary sequence residues of Cx32 obtained from the PDB database were used for comparative modeling, and the most favorable template was a Gap junction beta-2 protein of connexin-32 gap junction channel (PDB accession code 5KK9), a homodimer of a sequence identity of 63.68% with the connexin-26 gap junction channel. Using PyMOL, both mutations were predicted to cause hydrogen bond losses as leucine would be substituted to proline at positions 79 and 155. In the diagram that depicted the interaction among the residues at codon 79 before and after the mutation, the hydrogen bond between p.L79 and p.75R was revealed to be under the influence (2.9A) (Figure 4a and 4b). As for the p.L155P mutation, it could result in the loss of hydrogen bonds simultaneously with Tyr151 and Val152 (Figure 4c and 4d). Thus, both mutations possibly perturbed the amino acid side chains and potentially modified the function of the altered gene products by modifying the number of H-bonds, so as to alter the channel characteristics of Cx32.

DISCUSSION

Twenty-eight non-related CMT patients from a research center in northern China were recruited

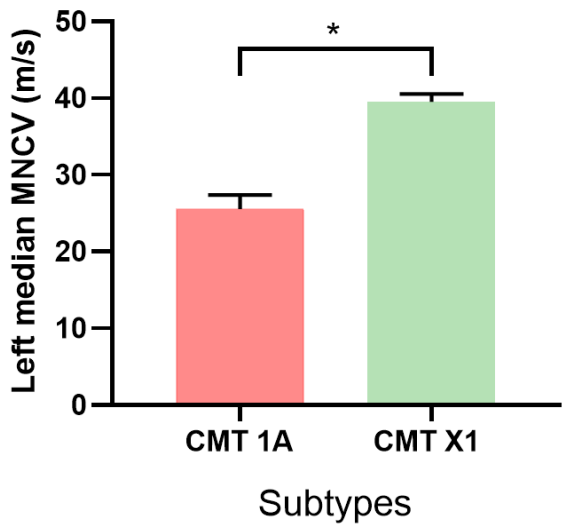

Figure 2. The analysis results of median nerve MNCV between 8 CMT1A patients and 3 CMTX1 patients.

Table 3: Electrophysiological characteristics of CMT patients carrying *PMP22 (dup)* mutations and novel *GJB1* mutations

Patient ID	Gene	Variants	Age	Gender	Median DML	Median MNCV	Median CMAP	Ulnar DML	Ulnar MNCV	Ulnar CMAP	Tibial DML	Tibial MNCV	Tibial CMAP	Common Peroneal DML	Common Peroneal MNCV	Common Peroneal CMAP	Median SNCV	Median SNAP amp	Ulnar SNCV	Ulnar SNAP amp	Sural SNAP amp
1	*PMP22*	Dup	59y	Male	8.71	30.6	4.1	4.79	27.2	6.4	7.12	/	2.2	5.72	20.2	4.8	22	4.4	33.4	1.9	/
2	*PMP22*	Dup	37y	Male	11.6	20.4	3.7	8.15	25.2	4.3	6.74	17.1	0.54	9.11	22.3	0.23	30.3	3	26.3	1.77	/
3	*PMP22*	Dup	58y	Male	6.16	28.6	3.2	5.47	25.2	3.2	/	/	/	8.08	22.7	0.03	/	/	/	/	/
4	*PMP22*	Dup	39y	Male	7.71	31.6	5.4	5.36	25.2	4.3	5.4	/	4.3	7.36	20.8	4.3	18.2	1.76	17.6	1.52	2.6
5	*PMP22*	Dup	28y	Female	9.31	26	4.3	6.02	23.7	2.2	6.09	0.53	/	13.3	/	/	30.4	1.32	/	/	/
6	*PMP22*	Dup	47y	Male	9.63	20.7	0.45	6.13	25.7	1.04	/	/	/	/	/	/	/	/	/	/	/
7	*PMP22*	Dup	13y	Male	8.6	21.1	10.2	5.27	19	4.3	8.32	18.7	0.42	8.4	16.9	0.21	23.4	1.4	22.1	0.9	/
Patient 1's daughter	*PMP22*	Dup	27y	Female	7.54	22.8	8	6.27	30	4.4	5.65	26.9	5.7	8.65	20.3	2	21.5	1.86	39.4	1.89	/
9	*GJB1*	c.464T>C p. L155P	17y	Male	4.71	40.1	1.06	3.05	34.7	1.32	6.48	/	0.059	/	/	/	30	4.9	34.8	1.96	/
Patient 9's mother	*GJB1*	c.464T>C p. L155P	40y	Female	3.96	42.6	6.2	2.56	43.2	8.8	3.98	/	6.5	3.24	38.7	1.28	31.2	2.95	36.1	1.86	/
10	*GJB1*	c.236T>C p. L79P	27y	Male	3.88	37.4	10	3.01	33.8	6.7	6.26	24.9	0.76	5.25	28.6	0.68	33.6	2.7	33	2.2	/

Abbreviations: amp = amplitude; CMAP = compound muscle action potential, amplitude in mV; CTMX1 = X-linked Charcot-Marie-Tooth disease type 1; DML = distal motor latency (ms); MNCV = motor nerve conduction velocity (m/s); SNAP = sensory nerve action potential, amplitude in μV; SNCV = sensory nerve conduction velocity (m/s); / = not detected or not measured.

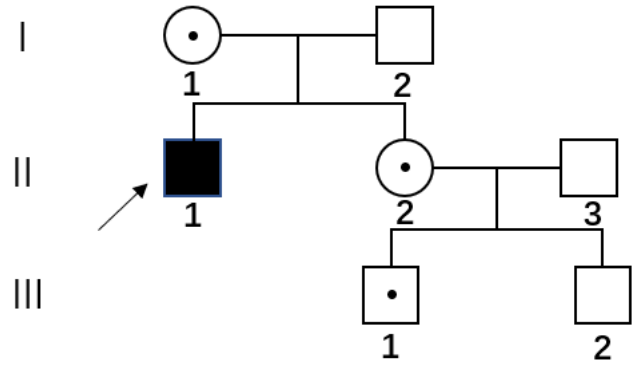

Figure 3. Pedigree structure of X-linked (CMTX6) kindred. Squares indicate males, circles indicate females. Solid symbols denote affected individuals and open symbols denote unaffected family members. Internal dots indicate obligate gene carriers.

for the study, and 18 patients had their DNA samples screened for mutations at several genes (*PMP22*, *MFN2, MPZ, GJB1*, and *GDAP-1*, etc.). Clinical manifestations and electromyography data of these CMT patients were recorded if available. Specifically, CMT1 was more prevalent than CMT2 in these patients, which was similar to the findings observed in large patient groups from other centers in China. Besides, *PMP22* duplication was the predominant mutation in these patients, followed by *GJB1* point mutations. By using MLPA assay combined with targeted NGS, the rate of genetic diagnosis for CMT grow to 77.8%. Whereas, some patients (4/18, 22.2%) still couldn't have their molecular mutations identified for diagnosis.

CMT clinical manifestations in this study were consistent with those reported previously. Distal weakness and atrophy were the most prevalent symptoms for these patients, followed by paresthesia and foot deformity. Among 8 CMT1A patients, 7 of them started with motor symptoms whereas only 1 started sensory symptoms. CMT1A accounts for nearly half of genetically confirmed

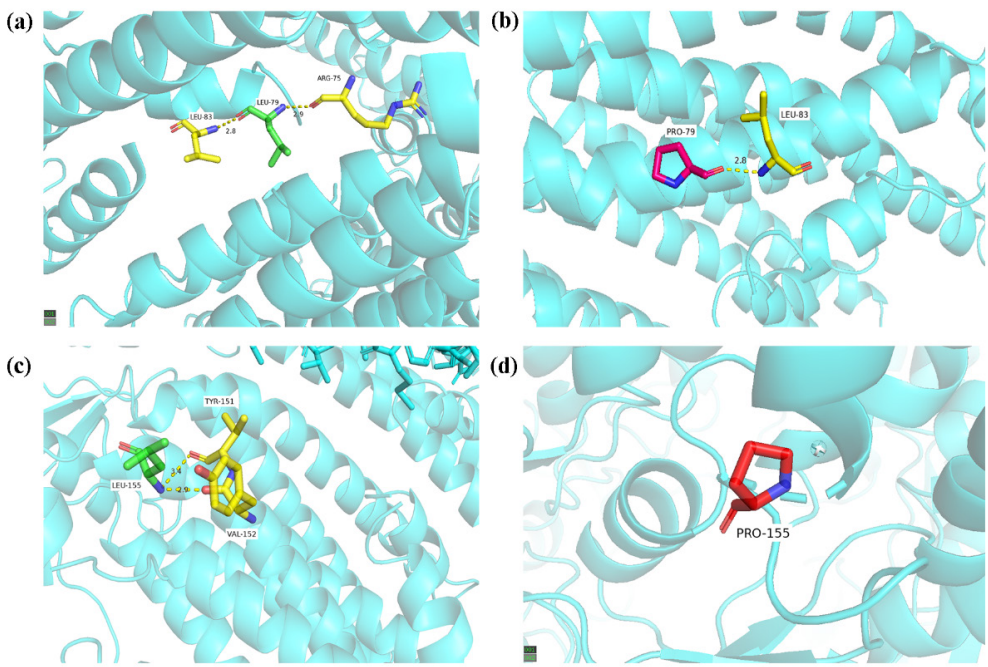

Figure 4. Mutation modelling. Diagram showing the interaction among the amino acid residues before (a) and after (b) the mutation at codon 79. The before and after mutation at codon 155 are showed in diagram (c) and (d). The loss of the H-bonds appears as a result of both the mutations.

cases, with the MNCVs between 20.4 m/s and 31.6 m/s. As a result, MLPA (*PMP22* duplication) should be the first mutation to assess not only for cases with MNCVs<25 m/s and a family history of autosomal dominance, but also for intermediate CMT patients (MNCV 25-45 m/s).

The highly conserved human microrchidia CW-type zinc finger 2 (*MORC2*) protein is predominantly expressed in the nucleus. It could promote chromatin remodeling in the regulation of DNA repair and transcription. In our series, we detected one 26-year-old CMT2Z patient with the known *MORC2* mutation (c.1396G>A; p.D466N). He was affected since childhood, showing poor walking, running and jumping than his peers. Both the proband's father and aunt had similar symptoms. Physical examination results suggested that atrophy and weakness of distal limbs and proximal were relatively reserved (distal lower limbs: 2/5, distal upper limbs: 4/5). Bilateral light touch sensation and vibration sensation existed symmetrically. The tendon reflexes generalized decreased. No pathologic reflexes or dystonia were observed. Besides, an elevation in serum creatine kinase (CK) level (983U/L, normal range: 50-310 U/L) was found via laboratory testing. Moreover, electrophysiological examinations showed remarkably lower CMAP amplitudes with normal MNCVs and unavailable SNAPs. Needle electromyography revealed frequent spontaneous muscular activity. Muscle magnetic resonance imaging (MRI) of lower limbs revealed fatty substitution and atrophy dominantly in distal region, which was concordant with the clinical examinations. In terms of myocardial involvement, the cardiac ultrasound showed ventricular septal hypertrophy. The 24-hour dynamic electrocardiogram showed that tachycardia events (heart rate > 120 bpm) accounted for 2.8% of the total heart beats. A pervious study of 14 patients with *MORC2* mutations showed serum creatine kinase levels were increased in 50%, but the reason was not clarified. We speculated that the increase of CK level may due to secondary muscle injury. The proband was different from previous reports with proximal limbs relatively reserved, but may be invloved as the disease progresses. In our study, the patient presented with heart involvement including heart structure and electrophysiology. His father with similar symptoms died of cardiac disease, which was not reported before. The cause of cardiac involvement requires more investigation and it might be one of the clinical characteristics of *MORC2*-related neuropathies.

Up to 10% of all CMT cases are categorized as X-linked CMT (CMTX), and CMT1X, caused by *GJB1* (Gap junction protein beta-1, also known as Cx32) gene mutations, is the most common subtype. Up to now, more than 450 different mutations have been identified on *GJB1* gene to affect all regions of the result protein. Although there have been many functional studies on *GJB1* mutations, how *GJB1* mutations cause CMT1X remains less fully understood. Most *GJB1* mutations lead to function loss in myelinating Schwann cells. According to previous research, most CMT1X cases can be distinguished from CMT1A ones with median nerve MNCVs. In this study, male CMT1X patients exhibited the median nerve MNCVs of 37.4 and 40.1 m/s respectively; for female CMT1X patients, the MNCV was 42.6 m/s. CMT1X patients generally demonstrate ''intermediate' drop of nerve conduction velocities and a mild prolongation of F-wave and distal motor latencies. In this series, all three patients had MNCVs of 25-45 m/s. Therefore, for patients with median nerve MNCVs (25-45 m/s) but no evidence of male-to-male transmission, *GJB1* mutations should be tested primarily. Additionally, the CMT1X phenotype is characterized by a combination of axonal and demyelinating features, and heterozygous women are either asymptomatic or less affected compared to men at all stages. In our study, patients carrying *GJB1* mutations all started with motor symptoms manifesting as gait disorder since childhood including unsteady walking and inability to walk on the heel. CNS involvement is a typical manifestation of CMT1X; however, no patient in our cohort exhibited paroxysmal dysphasia or white matter demyelination. The 2 novel mutations found in the study were located in the second and third transmembrane domains. In the molecular modeling of the two mutations, both mutations altered the amino acid sequence. They possibly perturbed the amino acid side chains and modified the functions of the altered gene product by changing the number of H-bonds, so as to alter the channel characteristics of Cx32. According to Mario Bortolozzi's review, CMT1X-related Cx32 mutations could lead to a plethora of alterations in the product proteins, including loss of channel formation, altered permeation properties, and defective gating mechanisms. But there is no research related to the mutation sites reported in our study and further verification is needed.

In addition to CMT1X, another case of CMTX6 was reported in our study. The pyruvate

dehydrogenase kinase isoenzyme 3 (*PDK3*) is a nuclear-encoded isoenzyme located in the mitochondrial matrix that regulates the pyruvate dehydrogenase complex (PDC) by reversible phosphorylation. Specifically, PDC is involved in the oxidative decarboxylation of pyruvate to acetyl CoA, connecting glycolysis to the lipogenic pathways and Krebs cycle as a key enzyme. In 2013, Kennerson *et al*. identified a missense *PDK3* gene mutation (p.R158H) for the first time in an Australian family by linkage analysis and WES. They found that such a mutation led to CMTX6 in the family, and the R158H-mutated *PDK3* confered enzyme hyperactivity and demonstrated stronger affinity to the inner-lipoyl (L2) domain of PDC's E2p chain than the wild-type. Later in 2016, the same group of researchers identified a Korean CMTX6 family with the same *PDK3* mutation from a 746 CMT cohort. Clinical, electrophysiological and neuroimaging observations from the Korean CMTX6 family with the p.R158H mutation were similar to the axonal neuropathy results revealed in the Australian family. No other patients have been described for *PDK3* mutations. Here, we confirmed the first Chinese CMTX6 patient with a p.R158H *PDK3* mutation. The proband in our study presented with weakness in both lower limbs, predominantly in the distal extremities, accompanied by steppage gait and reduced tendon reflexes. According to pervious reports, the lower extremities tend to be involved early and be more severely affected than the upper ones. Our results were consistent with previously reports. The proband's mother and sister were both carriers of the mutation but were asymptomatic and able to walk without assistance. Our study further supports that the p.R158H mutation may be an important spot for CMTX6. Since such a mutation is rare in populations, relevant unsolved CMT patients may need to be followed up for its prevalence.

While there are some interesting observations and findings to be drawn from this study, there were some limitations. First, the relatively small number of patients place limitation to the generalization of these results. Second, there are still a considerable number of patients do not have the opportunity to receive genetic examination, which affect the estimated positive rate of the genetic examination. In addition, the physical examination and auxiliary examination of CMT recruits should be further improved. In the future, we will continue to include more CMT recruiters to enrich the clinical phenotypes and genetic causes of CMT.

In conclusion, this study provided a general perspective of the clinical manifestations and genetic subtype frequencies in CMT patients treated at a medical center in Taiyuan, Northern China. Similar to previous literature, the most common CMT type in our center was CMT1A, followed by CMT1X. Moreover, 2 de novo *GJB1* mutations were found in two families and had expanded the spectrum of pathogenic mutations in CMT1X. In addition, we confirmed the first Chinese CMTX6 patient with a p.R158H *PDK3* mutation. Despite the growing popularity of NGS, Chinese CMT patient cohorts remain rarely screened genetically with NGS. Comprehensive clinical documentations can boost the chance to detect causative mutations, and a fundamental for subsequent genetic testing strategies should be electromyography data. However, there is still a large proportion of clinically diagnosed CMT patients who do not receive a genetic diagnosis. Our results have broadened the understanding of the genetic and clinical spectra of CMT patients, thereby assisting in the optimization of genetic and clinical diagnosis procedures. If MLPA technique is combined with target NGS, the success rate for CMT genetic diagnosis will consequently rise.

DISCLOSURE

Data availability: All data generated or analysed during this study are included in this published article [and its supplementary information files]. All data are available from the corresponding author on reasonable request.

Supplementary material: Supplementary Table 1 demonstrates the panel of 197 genes that have been known to participate in the pathology of CMT and several other inherited peripheral neuropathies.

Conflict of interest: None

REFERENCES

1. "2nd Workshop of the European Cmt Consortium: 53rd Enmc International Workshop on Classification and Diagnostic Guidelines for Charcot-Marie-Tooth Type 2 (Cmt2-Hmsn Ii) and Distal Hereditary Motor Neuropathy (Distal Hmn-Spinal Cmt) 26-28 September 1997, Naarden, the Netherlands." *Neuromuscul Disord* 1998; 8(6): 426-31. https://www.ncbi.nlm.nih.gov/pubmed/9713862.
2. Barisic N, Claeys KG, Sirotkovic-Skerlev M, *et al*. Charcot-Marie-Tooth disease: A clinico-genetic confrontation. *Ann Hum Genet* 2008;72(Pt 3): 416-41. doi:10.1111/j.1469-1809.2007.00412.x.
3. Berciano J, Garcia A, Gallardo E, *et al*. Intermediate Charcot-Marie-Tooth disease: An electrophysiological

reappraisal and systematic review. *J Neurol* 2017; 264(8): 1655-77. doi:10.1007/s00415-017-8474-3.
4. Bortolozzi M. What's the function of connexin 32 in the peripheral nervous system? *Front Mol Neurosci* 2018;11: 227. doi:10.3389/fnmol.2018.00227.
5. Chen CX, Dong HL, Wei Q, *et al*. Genetic spectrum and clinical profiles in a Southeast Chinese cohort of Charcot-Marie-Tooth disease. *Clin Genet* 2019; 96(5): 439-48. doi:10.1111/cge.13616.
6. Dubourg O, Tardieu S, Birouk N, *et al*. Clinical, electrophysiological and molecular genetic characteristics of 93 patients with X-linked Charcot-Marie-Tooth disease. *Brain* 2001;124(Pt 10): 1958-67. doi:10.1093/brain/124.10.1958.
7. Gutmann L, Shy M. Update on Charcot-Marie-Tooth disease. *Curr Opin Neurol* 2015;28(5): 462-7. doi:10.1097/WCO.0000000000000237.
8. Hahn AF, Brown WF, Koopman WJ, Feasby TE. X-linked dominant hereditary motor and sensory neuropathy. *Brain* 1990;113 (Pt 5): 1511-25. doi:10.1093/brain/113.5.1511.
9. He J, Guo L, Xu G, *et al*. Clinical and genetic investigation in Chinese patients with demyelinating Charcot-Marie-Tooth disease. *J Peripher Nerv Syst* 2018;23(4): 216-26. doi:10.1111/jns.12277.
10. Karadima G, Koutsis G, Raftopoulou M, Floroskufi P, Karletidi KM, Panas M. Four novel connexin 32 mutations in X-linked Charcot-Marie-Tooth disease. Phenotypic variability and central nervous system Involvement." *J Neurol Sci* 2014;341(1-2): 158-61. doi:10.1016/j.jns.2014.04.007.
11. Kennerson ML, Kim EJ, Siddell A, *et al*. X-linked Charcot-Marie-Tooth disease type 6 (Cmtx6) patients with a P.R158h mutation in the pyruvate dehydrogenase kinase isoenzyme 3 gene. *J Peripher Nerv Syst* 2016;21(1): 45-51. doi:10.1111/jns.12160.
12. Kennerson ML, Yiu EM, Chuang DT, *et al*. A new locus for X-linked dominant Charcot-Marie-Tooth disease (Cmtx6) is caused by mutations in the pyruvate dehydrogenase kinase isoenzyme 3 (Pdk3) gene. *Hum Mol Genet* 2013;22(7): 1404-16. doi:10.1093/hmg/dds557.
13. Kleopa KA, Abrams CK, Scherer SS. How do mutations in Gjb1 cause X-linked Charcot-Marie-Tooth disease?, *Brain Res* 2012;1487: 198-205. doi:10.1016/j.brainres.2012.03.068.
14. Korotchkina LG, Patel MS. Site specificity of four pyruvate dehydrogenase kinase isoenzymes toward the three phosphorylation sites of human pyruvate dehydrogenase. *J Biol Chem* 2001;276(40): 37223-9. doi:10.1074/jbc.M103069200.
15. Li DQ, Nair SS, Ohshiro K, *et al*. Morc2 signaling integrates phosphorylation-dependent, atpase-coupled chromatin remodeling during the DNA damage response. *Cell Rep* 2012;2(6): 1657-69. doi:10.1016/j.celrep.2012.11.018.
16. Mathis S, Goizet C, Tazir M, *et al*. Charcot-Marie-Tooth diseases: An update and some new proposals for the classification. *J Med Genet* 2015;52(10): 681-90. doi:10.1136/jmedgenet-2015-103272.
17. Nicholson G, Myers S. Intermediate forms of Charcot-Marie-Tooth neuropathy: A review. *Neuromolecular Med* 2006;8(1-2): 123-30. doi:10.1385/nmm:8:1-2:123.
18. Pareyson D, Marchesi C. Diagnosis, natural history, and management of Charcot-Marie-Tooth disease. *Lancet Neurol* 2009;8(7): 654-67. doi:10.1016/S1474-4422(09)70110-3.
19. Patel MS, Nemeria NS, Furey W, Jordan F. The pyruvate dehydrogenase complexes: Structure-based function and regulation. *J Biol Chem* 2014;289(24): 16615-23. doi:10.1074/jbc.R114.563148.
20. Phillips LH, Kelly TE, Schnatterly P, Parker D. Hereditary motor-sensory neuropathy (Hmsn): Possible X-linked dominant inheritance. *Neurology* 1985;35(4): 498-502. doi:10.1212/wnl.35.4.498.
21. Reilly MM, Murphy SM, Laura M. Charcot-Marie-Tooth disease. *J Peripher Nerv Syst* 2011;16(1): 1-14. doi:10.1111/j.1529-8027.2011.00324.x.
22. Rozear MP, Pericak-Vance MA, Fischbeck K, *et al*. Hereditary motor and sensory neuropathy, X-linked: A half century follow-up. *Neurology* 1987;37(9): 1460-5. doi:10.1212/wnl.37.9.1460.
23. Semplicini C, Ollagnon-Roman E, Leonard-Louis S, *et al*. High intra-familiar clinical variability in Morc2 mutated Cmt2 patients. *Brain* 2017;140(4: e21. doi:10.1093/brain/awx019.
24. Shi J, Zhao F, Pang X, *et al*. Whole-exome sequencing identifies a heterozygous mutation in Slc12a6 associated with hereditary sensory and motor neuropathy. *Neuromuscul Disord* 2021;31(2): 149-57. doi:10.1016/j.nmd.2020.11.002.
25. Shy ME, Siskind C, Swan ER, *et al*. Cmt1x phenotypes represent loss of Gjb1 gene function. *Neurology* 2007;68(11): 849-55. doi:10.1212/01.wnl.0000256709.08271.4d.
26. Sivera R, Lupo V, Frasquet M, *et al*. Charcot-Marie-Tooth disease due to Morc2 mutations in Spain. *Eur J Neurol* 2021;28(9): 3001-11. doi:10.1111/ene.15001.
27. Skre H. Genetic and clinical aspects of Charcot-Marie-Tooth's disease. *Clin Genet* 1974;6(2): 98-118. doi:10.1111/j.1399-0004.1974.tb00638.x.
28. Stenson PD, Mort M, Ball EV, Shaw K, Phillips A, Cooper DN. The human gene mutation database: Building a comprehensive mutation repository for clinical and molecular genetics, diagnostic testing and personalized genomic medicine. *Hum Genet* 2014;133(1): 1-9. doi:10.1007/s00439-013-1358-4.
29. Sun B, Z. Chen Z, Ling L, Yang F, Huang X. Clinical and genetic spectra of Charcot-Marie-Tooth disease in Chinese Han patients. *J Peripher Nerv Syst* 2017;22(1): 13-8. doi:10.1111/jns.12195.
30. Wang R, He J, Li JJ, *et al*. Clinical and genetic spectra in a series of Chinese patients with Charcot-Marie-Tooth disease. *Clin Chim Acta* 2015;451(Pt B): 263-70. doi:10.1016/j.cca.2015.10.007.
31. Zhao X, Li X, Hu Z, *et al*. Morc2 mutations in a cohort of Chinese patients with Charcot-Marie-Tooth disease Type 2. *Brain* 2016;139(Pt 10): e56. doi:10.1093/brain/aww156.

Supplementary table 1: genes in CMT NGS panels in our study.

CMT genes sequenced and analyzed
AAAS AARS1 AASS ABAT ABCA1 ABCD1 ABHD12 ACAT1 ACBD5 ACER3 ACO2 ACOX1 ACOX2 ACTA1 ACTN2 ACY1 ADA2 ADCY6 ADK ADPRS AFG3L2 AGA AGK AGL AGTPBP1 AHDC1 AIFM1 AIMP1 ALDH18A1 ALS2CL AMACR AMN AMPD2 AMT ANTXR2 AP1S1 AP1S2 AP5Z1 APOB APTX AR ARG1 ARHGDIA ARHGEF10 ARHGEF2 ARL6IP1 ARSA ARSB ARSL ARV1 ASAH1 ASCC1 ASL ASNS ASP A ASPM ASS1 ASXL1 ASXL2 ASXL3 ATAD3A ATL1 ATL3 ATP13A2 ATP1A1 ATP1A3 ATP6AP1 ATP6AP2 ATP7A ATP7B AUH AUTS2 B4GALNT1 B4GAT1 BAG3 BCAP31 BCKDHA BEAN1 BICD2 BIN1 BRAT1 BSCL2 BUB1B C12orf4 C12orf65 C19orf12 C1orf194 CA2 CACNA1A CACNA1D CACNA1G CACNA1S CANT1 CAPN1 CARS2 CAV1 CCBE1 CCDC115 CCDC174 CCDC47 CCDC78 CCDC88A CCDC88C CCND1 CCT5 CD59 CDC45 CDC6 CDCA7 CDK5RAP2 CDKAL1 CDKN1C CDT1 CENPF CENPJ CEP120 CEP135 CEP152 CEP164 CEP19 CEP41 CEP55 CEP57 CEP63 CEP85L CERT1 CFL2 CHCHD10 CHD1 CHD7 CHN1 CHP1 CIC CILK1 CKAP2L CLCF1 CLCN7 CLN3 CLN5 CLN6 CLP1 CNTNAP1 CNTNAP2 COA7 COASY COG7 COL6A1 COL6A2 COL6A3 COLQ COMP COQ2 COQ4 COQ6 COQ7 COQ8A COQ9 COX6A1 CP CPLX1 CPOX CPT1A CPT1C CPT2 CRAT CRBN CRIPT CRLF1 CRPP A CSNK2A1 CSNK2B CSPP1 CTDP1 CTSD CTU2 CUBN CUL4B CWF19L1 CYB5R3 CYFIP2 CYP27A1 CYP2U1 CYP7B1 D2HGDH DAG1 DARS2 DCAF8 DCTN1 DDHD1 DEAF1 DEGS1 DGAT2 DGUOK DHCR7 DHFR DHH DHPS DHTKD1 DHX16 DLL1 DMD DMXL2 DNAJB2 DNAJC3 DNM1L DNM2 DNMT1 DOCK3 DOLK DONSON DP AGT1 DPYS DRP2 DSE DST DSTYK DUOXA2 DYNC1H1 DYNC2I2 DYRK1A EBP ECM1 EDC3 EEF1A2 EFL1 EGR2 EIF2S3 ELOVL4 ELOVL5 ELP1 EMC1 EPG5 EPRS1 ERCC1 ERCC3 ERCC6 ERCC6L2 ERCC8 ERLIN2 ERMARD ETHE1 EVC EXOSC3 EXOSC9 EXT1 EXT2 F AH F AM126A F AM149B1 F ASTKD2 FBLN5 FBN1 FBXO38 FBXW11 FCSK FDFT1 FDX2 FGD4 FGF14 FH FHL1 FIBP FIG4 FITM2 FKRP FKTN 7/29 FLNC FLVCR1 FOLR1 FRRS1L FUCA1 FXN FXR1 FXYD2 GAA GAD1 GALC GALK1 GAN GARS1 GATM GBA2 GBE1 GCK GCLC GDAP1 GDI1 GEMIN4 GFM1 GFM2 GJB1 GJB3 GJC2 GLA GLE1 GLUD1 GLUL GM2A GMNN GMPP A GMPPB GNA11 GNAS GNB4 GNE GNP AT GNPTG GOT2 GPHN GPI GPT2 GRIA3 GRN GTPBP2 GTPBP3 GUCY1A1 GUF1 H1-4 H19 HAAO HADH HADHA HAL HARS1 HAX1 HEPHL1 HEXA HFE HGSNAT HIBCH HIKESHI HINT1 HK1 HMBS HMGCL HNRNP A2B1 HOXD10 HPD HPRT1 HSD17B4 HSPB1 HSPB3 HSPB8 HYLS1 IARS2 IBA57 IER3IP1 IFRD1 IGHMBP2 INF2 INS IRAK4 IREB2 IRF2BPL ISG15 ITP A IYD JAG1 JAM2 JPH1 KARS1 KATNIP KCNA1 KCND3 KCNJ10 KCNJ18 KIAA0586 KIAA0753 KIAA1109 KIF1A KIF1B KIF5A KIFBP KLC2 KLHL9 KYNU LAMA2 LAMB2 LAS1L LDB3 LEP LGI4 LIFR LINGO1 LINS1 LIPT1 LIPT2 LITAF LMAN2L LMBRD1 LMNA LNPK LOX LRP12 LRP4 LRSAM1 LSS LYST LZTFL1 MAB21L1 MAG MANBA MAOA MAP3K20 MAPK8IP3 MARCHF6 MARS1 MAT1A MATR3 MBTPS2 MCCC2 MCIDAS MCM3AP MDH2 MECR MED25 MEGF10 MESD MFF MFN2 MFSD2A MFSD8 MGME1 MICU1 MLC1 MLYCD MMAA MMACHC MME MMUT MN1 MOCS2 MORC2 MPC1 MPI MPLKIP MPV17 MPZ MRE11 MRPS34 MSTO1 MTFMT MTHFR MTHFS MTMR2 MTO1 MTR MTRR MTTP MVK MYBPC1 MYD88 MYH14 MYL1 MYO1F MYORG MYOT NAGA NAGLU NALCN NANS NARS2 NAXD NAXE NCAPD3 NDRG1 NDUF A1 NDUF A9 NEB NECAP1 NEFH NEFL NEK1 NEPRO NEXMIF NF2 NF ASC NGF NGLY1 NHLRC2 NKAP NKX6-2 NLGN4X NOG NOVA2 NPC1 NPC2 NRROS NRXN1 NTNG2 NTRK1 OFD1 OP A1 OP A3 ORAI1 OSTM1 OTC OXR1 P4HTM P ACS1 P ACS2 P AH P AK3 P AX7 PCBD1 PCK1 PCNT PCYT2 PDCD1 PDGFB PDGFRA PDK3 PDSS1 PDSS2 PDXK PDYN PEPD PEX1 PEX10 PEX11B PEX12 PEX16 PEX2 PEX3 PEX5 PEX7 PGAP1 PGAP2 PGAP3 PGK1 PGM3 PHGDH PHKG2 PHYH PIBF1 PIEZO2 PIGA PIGB PIGG PIK3R5 PKDCC PLA2G6 PLD3 PLEKHG5 PLG PLK4 PLP1 PLPBP PMM2 PMP2 PMP22 PMPCA PNKP PNP PNPLA2 PNPLA6 PNPO PNPT1 POLG POLR3A 8/29 POMGNT1 POMK POP1 PP A2 PPOX PRDM12 PREPL PRICKLE1 PRKAR1A PRKCG PRNP PRODH PRPS1 PRUNE1 PRX PSAP PSAT1 PSEN2 PTCH1 PTDSS1 PTRH2 PTS PURA PYCR1 PYROXD1 QRICH1 RAB18 RAB3GAP1 RAB7A RAI1 RALGAP A1 RBM28 REEP1 REEP2 RELN RETREG1 RFT1 RIPPLY2 RMND1 RMRP RNASEH1 RNASEH2A RNASEH2C RNASET2 RNF170 ROGDI RPE65 RPIA RRM2B RSRC1 RTN2 RTN4IP1 RUBCN RUNX2 RUSC2 RYR1 SACS SAMD9L SAR1B SASS6 SBDS SBF1 SBF2 SC5D SCN10A SCN11A SCN9A SCO2 SCP2 SCYL1 SCYL2 SEC61A1 SEMA3E SEPTIN9 SERPING1 SERPINI1 SETX SGCA SGCE SGMS2 SGPL1 SH3PXD2B SH3TC2 SHANK3 SIGMAR1 SIK1 SIL1 SLC12A6 SLC25A1 SLC25A15 SLC25A19 SLC25A21 SLC25A4 SLC25A46 SLC2A1 SLC30A10 SLC35A1 SLC46A1 SLC52A2 SLC52A3 SLC5A6 SLC5A7 SLC6A19 SLC9A1 SMCHD1 SMN1 SMPD1 SMPD4 SMS SNAP25 SNAP29 SNX14 SOBP SORD SOX10 SP ART SP AST SPECC1L SPEG SPG11 SPG21 SPTBN2 SPTBN4 SPTLC1 SPTLC2 SQSTM1 SSR4 ST3GAL5 STAC3 STAMBP STIL STRA6 STRADA STUB1 STXBP1 SUCLA2 SUCLG1 SUFU SUMF1 SUOX SURF1 SVBP SYNE1 SYT2 SZT2 TALDO1 TASP1 TAZ TBC1D20 TBC1D23 TBC1D24 TBCE TBCK TBL1XR1 TCF20 TCN2 TCTN1 TDP1 TDP2 TECPR2 TERT TF AP2B TFG TG TH THG1L THRA TIMM8A TIMMDC1 TKFC TKT TLK2 TM4SF20 TMEM106B TMEM107 TMEM126A TMEM138 TMEM165 TMEM216 TMEM237 TMEM240 TMEM260 TMEM63A TNFRSF1 1A TOE1 TOP3A TPI1 TPK1 TPM2 TPP1 TRAK1 TRIM2 TRIM32 TRIP4 TRMT5 TRNT1 TRPV4 TSFM TSPYL1 TTBK2 TTC19 TTR TUBB3 TUBGCP2 TUBGCP4 TUBGCP6 TWNK TXN2 TYMP TYROBP UBA1 UBA5 UCHL1 UFC1 UFM1 UGP2 UNC80 UPB1 UROC1 VAMP1 VANGL1 VAPB VCP VHL VIP AS39 VMA21 VPS13A VPS13C VPS13D VPS37A VPS45 VRK1 VWA3B WARS1 WASHC5 WFS1 WNK1 WWOX XK XRCC1 XRCC4 YAP1 YARS1 YY1AP1 ZC4H2 ZFHX2 ZFYVE26 ZIC1 ZSWIM6